Long-range corrected hybrid functionals for π-conjugated systems: Dependence of the range-separation parameter on conjugation length

Thomas Körzdörfer, John S. Sears, Christopher Sutton, and Jean-Luc Brédas

Citation: J. Chem. Phys. **135**, 204107 (2011); doi: 10.1063/1.3663856
View online: http://dx.doi.org/10.1063/1.3663856
View Table of Contents: http://jcp.aip.org/resource/1/JCPSA6/v135/i20
Published by the American Institute of Physics.

Long-range corrected hybrid functionals for π-conjugated systems: Dependence of the range-separation parameter on conjugation length

Thomas Körzdörfer, John S. Sears, Christopher Sutton, and Jean-Luc Brédas[a)]
School of Chemistry and Biochemistry and Center for Organic Photonics and Electronics, Georgia Institute of Technology, Atlanta, Georgia 30332-0400, USA

(Received 20 October 2011; accepted 4 November 2011; published online 30 November 2011)

Long-range corrected (range-separated hybrid) functionals represent a relatively new class of functionals for generalized Kohn-Sham theory that have proven to be very successful, for instance, when it comes to predicting ionization potentials and energy gaps for a wide range of molecules and solids. The results obtained from long-range corrected density functional theory approaches can be improved dramatically, if the range-separation parameter (ω) is optimized for each system separately. In this work, we have optimized ω for a series of π-conjugated molecular systems of increasing length by forcing the resulting functionals to obey the ionization potential-theorem, i.e., that their highest occupied eigenvalue be equal to the ΔSCF ionization potential. The optimized ω values are observed to vary substantially from their default values for the functionals. For highly conjugated chains such as oligoacenes and polyenes, we find that the characteristic length scale of the range-separation, i.e., $1/\omega$, grows almost linearly with the number of repeat units, for saturated alkane chains, however, $1/\omega$ quickly saturates after 5-6 repeat units. For oligothiophenes, we find that $1/\omega$ grows linearly for the shorter oligomers but then saturates at around 10 repeat units. Our results point to a close relation between the optimal range-separation parameter and the degree of conjugation in the system.
 [doi:10.1063/1.3663856]

I. INTRODUCTION

In recent years, the concept of range-separated hybrid functionals[1] has become increasingly exploited in the field of density functional theory (DFT).[2] The central idea in range-separated functionals is the partitioning of the Coulomb operator into short-range (SR) and long-range (LR) components, e.g., with the help of the standard error function (erf):

$$\frac{1}{r} = \frac{erf(\omega r)}{r} + \frac{erfc(\omega r)}{r}. \quad (1)$$

The error function provides only one of many possible range-separating functions that can be employed, although it does offer benefits for the computation of the electron-repulsion integrals over Gaussian basis sets. Researchers have also used, for instance, the Yukawa potential ($e^{-\omega r}$).[3–5] The range separation is determined in Eq. (1) by a single parameter ω, which is usually determined empirically, with $1/\omega$ defining a characteristic length scale for the transition between the SR and LR descriptions. Then, $1/2\omega$ corresponds to the distance at which the Coulomb operator transitions from being treated mostly by the SR description (*erfc*) to being treated mostly by the LR description (*erf*). Of central importance to the work presented here is that (as illustrated in Fig. 1) the characteristic length scale over which the treatment of the Coulomb operator changes from SR to LR increases with decreasing ω. Thus, the "optimal" range-separation parameter can be strongly dependent upon the length scales for electron correlation, a feature highlighted when considering the π-conjugated systems examined in this work.

By treating the SR and LR electron-electron interactions on a different footing, the range separation of the Coulomb operator allows one to benefit from the advantages of well-known semilocal approximations to exchange and correlation, while at the same time circumventing many of their shortcomings. In solids, for example, the range separation of the Coulomb operator allows one to effectively incorporate screening effects; at the same time, it leads to substantial computational savings and alleviates numerical difficulties that can arise due to the divergence of the Coulomb operator when including the full 1/r potential.[6–9] In molecular systems, on the other hand, the motivations for incorporating the range separation are slightly different. Here, we focus on this second type of range-separated functionals, which we refer to as long range-corrected (LRC) hybrids. These functionals employ full nonlocal Hartree-Fock (HF) exchange plus local correlation in the LR, while the nonclassical SR interaction is treated by standard semilocal or hybrid functionals. As a consequence, LRC-hybrids restore the correct 1/r-asymptotic description of the exchange-correlation potential (hence, the term "long-range corrected"), thereby improving the description of several molecular properties that are sensitive to such long-range interactions. Important examples of these include ionization potentials,[2] reaction barrier heights,[10,11] polarizabilities in large molecules,[12–14] nonlinear optical properties, as well as charge-transfer and Rydberg excitations.[15–17] Additional advantages of LRC-hybrids can arise from the details of their numerical treatment. Just as standard hybrid functionals, LRC-hybrids are usually implemented within the generalized Kohn-Sham (GKS) scheme[18] that, in contrast to standard Kohn-Sham (KS) implementations, allows for

a)Electronic mail: jean-luc.bredas@chemistry.gatech.edu.

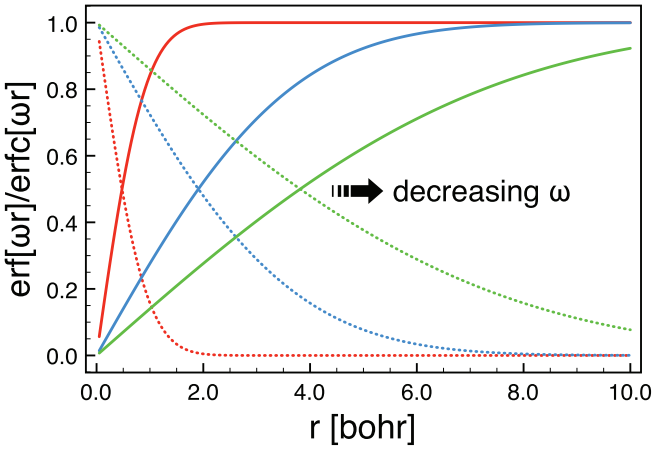

FIG. 1. Plot of *erf*(ωr) (solid lines) and *erfc*(ωr) (dashed lines) for ω equal to 1.0 bohr^{-1} (red), 0.25 bohr^{-1} (blue), and 0.125 bohr^{-1} (green).

nonlocal and orbital-dependent effective particle potentials. This implementation can substantially impact the obtained eigenvalues.[19] In particular and in contrast to standard KS theory, it becomes possible for the HOMO-LUMO gap obtained within an exact GKS treatment to equal the fundamental gap of the studied system when a suitable fraction of HF exchange is treated explicitly.[20,21] The LRC functionals incorporate a complete description of HF exchange at long range (and effectively on average incorporate a large percentage of the full HF exchange). As a consequence, GKS eigenvalues from LRC functionals can indeed satisfy the gap criterion when using the appropriate ω.[20,21]

As pointed out above, the main effect of the ω parameter is to control the length scale for range separation, i.e., for the screening of the Coulomb interaction, in the particular system of interest. It has been argued that the unknown "exact" ω is a functional of the density.[2] In practice, however, most LRC-hybrids employ a single constant value for ω, which is typically determined (semi-) empirically by fitting to a particular training set.[22] As a function of the optimization procedures and training sets employed as well as the underlying semilocal exchange-correlation functionals, typical ω values vary between 0.2 and 0.5 bohr^{-1}, thus covering characteristic separation lengths between 2 and 5 bohrs. However, since the optimal range-separation parameter has to reflect the Coulomb screening in the system of interest, it can be expected to be sensitive to the size and electronic structure of the system under study.

More recently, a number of different approaches have been developed to address this problem. Examples include LRC functionals with multiple ranges[23,24] as well as the so-called "local range-separated hybrids."[25–28] An alternative strategy has been considered in a number of recent investigations,[2,15–17,20,21,29] in which the range-separation parameter is optimized for each system of interest.

As for the latter, a frequently used approach is to determine ω by enforcing the DFT analog to Koopmans' theorem, i.e., by tuning ω such that the HOMO eigenvalue of the neutral system equals the ionization potential (IP), with the latter being determined as the difference in ground-state energies of the neutral ($E_{gs}(\omega,N)$) and cationic ($E_{gs}(\omega,N-1)$) systems. Consequently, the IP-optimized ω can be obtained by minimizing

$$\Delta_{IP}(\omega) = \left|\varepsilon_H^{\omega} - (E_{gs}(\omega, N) - E_{gs}(\omega, N-1))\right|. \quad (2)$$

Satisfying Eq. (2) defines a unique ω value that depends strongly on the electronic structure of the particular system and (to a lesser extent) on the choice of the semilocal functional. This "tuning" of ω is nonempirical and can be seen to impose a condition on the obtained functional to be satisfied in the limit of an exact KS (and GKS) approach.[2] A different interpretation of Eq. (2) is that, by minimizing $\Delta_{IP}(\omega)$, the so-called many-electron self-interaction error (MESIE) in the underlying density functionals is minimized as well.[2] The MESIE has been identified as responsible for many of the most severe failures of conventional density functionals.[30–32] Hence, it can be expected that the IP-optimization of LRC-hybrids not only improves those properties directly related to the IP, but also helps to solve other issues associated to the MESIE. However, the IP-fitting approach also comes with a severe drawback since, in a system formed by two molecules of a different nature, it is possible to optimize the IP of only one of them. This is due to the current limitation to a single global range-separation parameter. In principle, a balanced treatment could be restored by adopting a more flexible range-separation procedure, although in practice such a procedure could be difficult to implement.[33]

Earlier work has shown that the IP-optimized ω value (i) can differ substantially from the one determined by semi-empirical fitting and (ii) indeed displays a distinct dependency on system size.[15,16] Here, in order to better understand the size dependency of the optimized ω, we investigate how the IP-optimized ω values evolve with the number of repeat units in a series of molecular chains and how this evolution depends on conjugation.

II. METHODOLOGY

All the computations presented in this work on alkane, polyene, oligoacene, and oligothiophene chains were carried out with the QCHEM program package.[34] Ground-state geometries were optimized at the B3LYP/cc-pVTZ (Ref. 35) level. The IP-optimized ω values were obtained according to Eq. (2) in a series of calculations on the neutral and cationic molecules by varying the range-separation parameter in steps of 0.001 bohr^{-1}. A cc-pVDZ basis was employed for all the ω-optimizations presented here. For some of the smaller molecules we also employed a cc-pVTZ basis to check for basis-set convergence; in all cases, the basis-set dependence of the optimized ω was found to be inferior to 0.005 bohr^{-1}. Three LRC-hybrid functionals were considered: the long-range corrected Baer, Neuhauser, and Livshits functional (LC-BNL),[36] the LRC-version of the screened Perdew, Burke, and Ernzerhof functional (LC-ωPBE),[10] and the corresponding hybrid version, LC-ωPBEh, that – in contrast to LC-ωPBE – contains 20% of SR HF-exchange in addition to the full LR HF exchange.[37] This choice of functionals allows us to study

the differences arising from various semilocal approximations for exchange and correlation as well as those due to using a hybrid instead of a purely semilocal functional in the SR part. To make sure that our conclusions can be carried forward to other LRC hybrids, we also checked some of our results with other LRC-hybrids such as LC-BOP (Refs. 38 and 39) and the LC-ωB97-series.[22,40]

III. RESULTS

A. Polyenes and alkane chains

Polyene chains represent prototypical π-conjugated systems and we begin our analysis by discussing the IP-optimized range-separation parameters for $C_{2n}H_{2n+2}$ chains with n = 1 to 25. As expected from previous results on optimally tuned LRC hybrids,[16,20,21] the IP-optimized ω values decrease with increasing chain length whatever the nature of the functional. This decrease is very significant since, in going from ethylene (n = 1) to the longest chain examined here (n = 25), the optimal ω value changes by a factor of 4. In an attempt to gain insight into the size dependence of ω, we have plotted the characteristic length of the SR/LR separation, i.e., $1/\omega$, as a function of the number of repeat units in Fig. 2. We find a very strong dependence of $1/\omega$ on chain length for all three functionals. While the optimized ω values for LC-ωPBE and LC-BNL only differ by a small constant shift, the curve for the LC-ωPBEh shows a much larger shift and also presents a different slope than that observed in the other functionals. As a general trend, the LC-ωPBEh IP-optimization results in larger values for $1/\omega$, i.e., smaller values for ω as compared to the two other LRC-hybrids. This finding can be rationalized by the fact that LC-ωPBEh already includes 25% HF exchange in the SR part, thus increasing the characteristic length of the SR/LR transition. The results for the linear polyene chains point out that: (i) the optimal range-separation parameter strongly depends on the system size, and (ii) in such highly conjugated systems, the characteristic length scale for range separation has not converged even after 25 double bonds.

In order to explore to what extent conjugation plays a role in this evolution for the polyenes, we have examined the progression of the IP-optimized ω with chain length in linear alkane chains $C_{2n}H_{4n+2}$ (where we have defined the repeat unit to be consistent with that from the polyene chains).

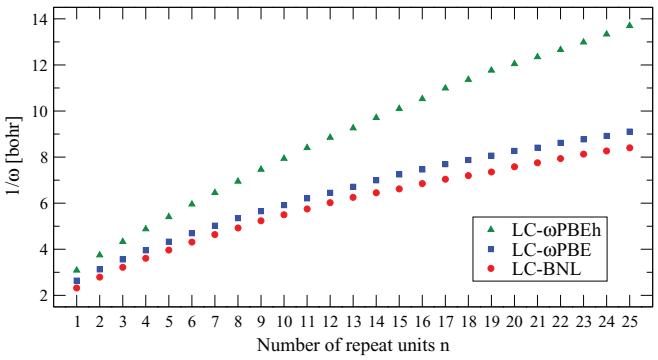

FIG. 2. IP-optimized SR/LR separation ($1/\omega$) for linear polyene chains $C_{2n}H_{2n+2}$ as a function of n.

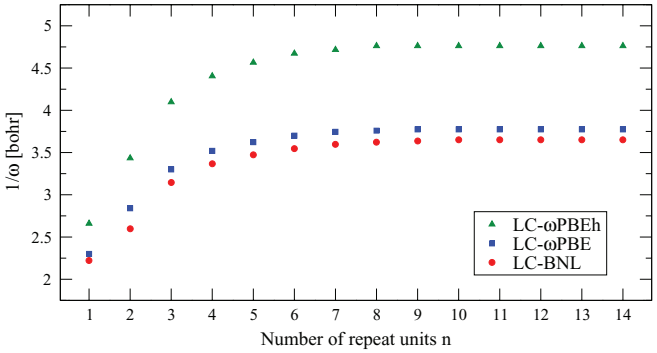

FIG. 3. IP-optimized SR/LR separation ($1/\omega$) for linear alkane chains $C_{2n}H_{4n+2}$ as a function of n.

The calculated characteristic lengths $1/\omega$ are plotted as a function of n in Fig. 3. For short chains (n$\sim$1-3), the evolution is nearly linear and similar to that observed for polyene chains. However, in contrast to what is observerd in polyene chains, the $1/\omega$ value saturates quickly and reaches a constant value ($\sim$3.75 bohrs) for n$\sim$7. This value is significantly smaller than those calculated for the polyene chains. Thus, not only the size but also the extent of conjugation plays an important role in determining the characteristic lengths.

To gain further insight, we have considered another example where conjugation is expected to play a dominant role in the modulation of ω and evaluated the impact of a torsion around the central C–C single bond in a long polyene chain, namely, $C_{24}H_{26}$. It is anticipated that conjugation will reduce as the conformation proceeds from planar to perpendicular and effectively cuts the molecule into two C_{12}-long conjugated segments. As can be observed from Fig. 4, the optimal separation distance $1/\omega$ decreases as π-conjugation along the polyene chain diminishes. The smallest $1/\omega$ is obtained at around a torsion angle of 90° and lies between the IP-optimized $1/\omega$ for the coplanar $C_{14}H_{16}$ and $C_{16}H_{18}$ chains, thus only slightly larger than the value found for the $C_{12}H_{14}$ chain. Interestingly, we find a small but noticable increase in $1/\omega$ between torsion angles of 85° and 90°, thus indicating an unexptected increase of conjugation. We conclude that this effect is triggered by an increase in the overlap of perpendicular p-orbitals at a torsion angle of exactly 90°.

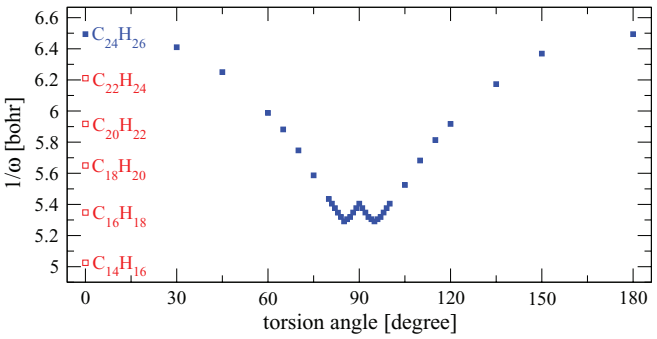

FIG. 4. IP-optimized SR/LR separation ($1/\omega$) for the torsion of $C_{24}H_{26}$ around the central C–C bond as a function of the torsion angle (filled blue squares). The red boxes along the left axis show the IP-optimized SR/LR lengths ($1/\omega$) for smaller polyenes with zero torsion angle for comparison.

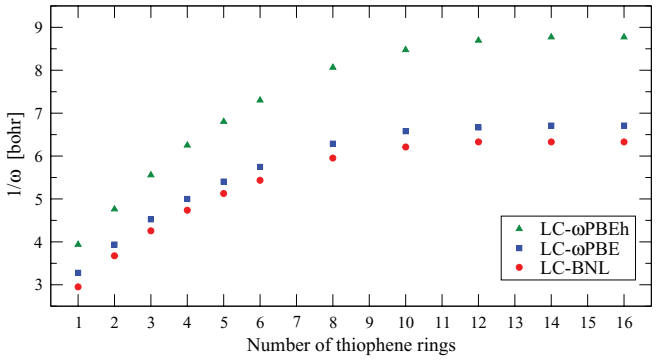

FIG. 5. IP-optimized SR/LR separation ($1/\omega$) for linear oligothiophenes as a function of the number of thiophene rings, n.

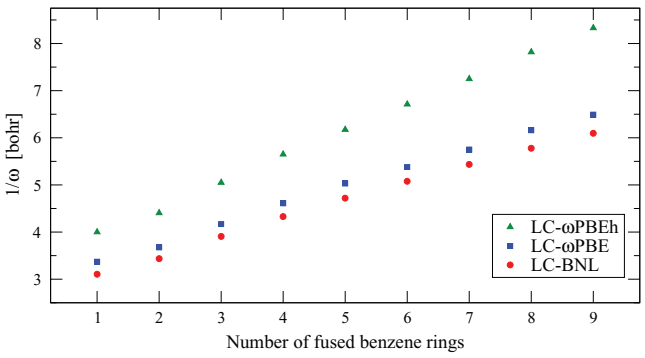

FIG. 6. IP-optimized SR/LR separation ($1/\omega$) for oligoacenes as a function of the number of fused benzene rings, n.

The comparison of the results for the polyene and alkane chains underscores that the characteristic length $1/\omega$ is sensitive not only to the size of the system but also, importantly, to the extent of conjugation. In this context, we now turn to two other types of conjugated systems, the oligothiophenes and oligoacenes, which are of high interest in the field of organic semiconductors.

B. Oligothiophenes and oligoacenes

Figure 5 displays the results for the IP-optimized SR/LR separation in oligothiophene chains containing up to n = 16 rings. A quasilinear progression of $1/\omega$ is observed for the shorter oligomers up to sexithienyl; saturation sets in at about n = 10. If we take account of only the C–C conjugated path along the oligomers, n = 10 rings correspond to 20 C–C double bonds. In comparison to the polyene series, saturation occurs at an earlier stage, which is consistent with the aromatic character of the oligothiophene molecules.

Based on DFT calculations at the B3LYP level, large unsubstituted acenes beyond hexacene have been predicted to display an antiferromagnetic open-shell singlet diradical ground state.[41] However, the question as to whether and at which length a transition occurs from closed-shell to open-shell ground states remains a controversial topic, particularly since the results can be expected to be significantly influenced by the level of theory.[42,43] As a result, we have chosen here to limit our discussion to oligoacenes up to nonacene and to treat the electronic ground states of all oligomers as closed-shell singlets. While the issues related to triplet instabilities in the acene series and the diradical character of long oligoacenes are beyond the scope of this work, they will be addressed in a separate study employing IP-optimized LRC-hybrid functionals. The results for oligoacenes containing up to n = 9 rings are given in Fig. 6.

Interestingly, the results show a clear linear progression with no sign of saturation for the longer acenes. If we assume that the closed-shell ground state extends beyond n = 9 rings, we actually find that the IP-optimized range-separation presents a linear progression through 20 repeat units without indication of a saturation onset. Considering that oligoacenes can be viewed as formed by two strongly coupled polyene chains running along the periphery of the oligomers, this observation is consistent with the results discussed above for the polyene chains.

To verify the generality of our results and make sure they are representative of all LRC-hybrid functionals irrespective of the underlying semilocal approximations, we carried out additional calculations with other LRC-hybrids including LC-BOP, LC-ωB97, LC-ωB97X, and LC-ωB97XD. The optimized ω values for these functionals follow exactly the same trend as for the LC-BNL and the LC-ωPBE functionals discussed above. While the IP-optimized ω values for LC-BOP and LC-ωB97 are generally close to the ones for LC-BNL and LC-ωPBE, those for LC-ωB97X and LC-ωB97XD are smaller and closer to the ones obtained for the LC-ωPBEh functional. This again reflects the fact that the introduction of fractional short-range Hartree-Fock exchange offsets the size-dependency-curve for the optimized ω values by a constant.

Importantly, the fact that the details of the underlying semilocal approximations to exchange and correlation do not significantly influence the evolution of the IP-optimized ω values with chain length highlights that the IP-optimized range-separation parameter captures the spatial extent of electronic coupling, i.e., an intrinsic property of the system of interest. It is thus not surprising that this concept can be related to what is typically referred to as conjugation length or chemical hardness/softness. As the IP-optimized ω value is fully derived from the electronic structure of the system and obeys constraints that are required from the exact functional, we believe that it has the potential to offer an alternative representation of the conjugation length that can be determined solely from first principles.

C. Evaluation of ionization potentials and fundamental energy gaps with IP-optimized functionals

We now comment on the actual performance of the IP-optimized LRC-hybrids for predicting the ionization potentials and fundamental energy gaps in oligoacenes. We note that the performance of the optimized LRC functionals has been addressed already by many authors,[11,14–16,20,21] and a detailed study of the benefits of these approaches is beyond the scope of this work. In Table I, we compare the HOMO eigenvalues obtained from the IP-optimized LRC-hybrids to experimental IPs as well as to the best available theoretical

TABLE I. HOMO eigenvalues from IP-optimized and standard LRC-hybrids as compared to experimental IPs,[46,47] adiabatic (AIP) and vertical (VIP) IPs from CCSD(T)/cc-pV∞Z calculations,[44] as well as HOMO eigenvalues from HF and B3LYP for oligoacenes from benzene ($n = 1$) to hexacene ($n = 6$). A cc-pVTZ basis set was employed in all HF and DFT calculations, while the CCSD(T) reference calculations used an extrapolated cc-pV∞Z basis. All values given in (eV).

Nb of repeat units	1	2	3	4	5	6
Expt. IP	9.24 (Ref. 46)	8.14 (Ref. 46)	7.42 (Ref. 47)	6.94 (Ref. 47)	6.59 (Ref. 47)	6.36–6.44 (Ref. 46)
AIP CCSD(T) (Ref. 44)	9.22	8.14	7.41	6.91	6.55	6.42
VIP CCSD(T) (Ref. 44)	9.44	8.24	7.47	6.95	6.57	6.43
$-\varepsilon_H$ IP-opt. LC-BNL	9.45	8.20	7.36	6.79	6.40	6.10
$-\varepsilon_H$ IP-opt. LC-ωPBE	9.36	8.15	7.32	6.77	6.38	6.09
$-\varepsilon_H$ IP-opt. LC-ωPBEh	9.30	8.10	7.28	6.73	6.35	6.05
$-\varepsilon_H$ stand. LC-BNL	9.96	8.76	7.98	7.45	7.06	6.77
$-\varepsilon_H$ stand. LC-ωPBE	9.81	8.64	7.89	7.37	7.00	6.73
$-\varepsilon_H$ stand. LC-ωPBEh	9.07	8.00	7.32	6.87	6.54	6.30
$-\varepsilon_H$ B3LYP	7.03	6.09	5.52	5.14	4.87	4.68
$-\varepsilon_H$ HF	9.13	7.87	7.03	6.46	6.04	5.73

estimates for the adiabatic and vertical IPs at a benchmark level of theory [estimated CCSD(T)/cc-pV∞Z]. For comparison, we also provide the HOMO eigenvalues from B3LYP, HF, and the LRC-hybrids that use the standard (empirically fitted) values for ω (i.e., 0.5 bohr^{-1} for LC-BNL, 0.4 bohr^{-1} for LC-ωPBE, and 0.2 bohr^{-1} for LC-ωPBEh). As the HOMO eigenvalues from (approximate) DFT are supposed to approximate vertical IPs, one should compare the calculated DFT eigenvalues to the vertical IPs from the CCSD(T) calculation.

From Table I, we conclude that the IP-optimized LRC-hybrids yield the best overall performance of all considered DFT methods, typically improving the B3LYP results by several eV. The comparison with the non-optimized LRC-hybrids further demonstrates the importance of the IP-fitting procedure. The example of benzene shows that standard LRC-hybrids can overestimate (LC-ωBNL) or underestimate (LC-ωPBEh) the vertical IP by nearly half an eV. In contrast, all IP-optimized LCR-hybrids yield very similar HOMO eigenvalues within 0.1 eV. The conclusions drawn from the IPs can also be carried forward to the fundamental energy gaps as illustrated in Fig. 7. The IP-optimized LRC-hybrids all show very similar gaps that compare favorably to the reference values with the latter corresponding to the differences between vertical IPs and vertical electron affinities (EAs) from highly accurate CCSD(T)/cc-pV∞Z calculations.[44,45] The optimized LRC-hybrids clearly outperform all widely used semilocal and hybrid functionals by several eV, thus yielding a workaround for the infamous gap-problem of DFT.[20] Importantly, in line with what was seen in the evolution of the characteristic lengths presented above, the results demonstrate that in the case of the IP-optimized LRC-hybrids the details of the underlying semilocal approximations to exchange and correlation only play a minor role as compared to the prominent impact of the range-separation parameter.

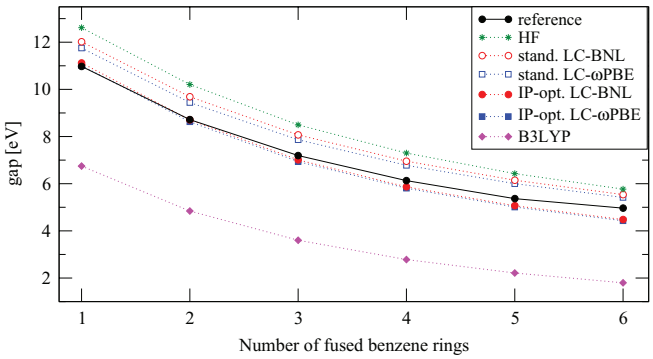

FIG. 7. Difference between highest occupied molecular orbital (HOMO) and lowest unoccupied molecular orbital (LUMO) eigenvalues from HF, standard- and IP-optimized LRC-hybrids, and B3LYP for oligoacenes from benzene (n = 1) to hexacene (n = 6) using a cc-pVTZ basis. The reference gap corresponds to differences between the vertical IP and vertical EA from CCSD(T)/cc-pv∞Z calculations.[44,45]

IV. CONCLUSIONS

In summary, we have calculated the IP-optimized range-separation parameters for alkanes, polyenes, oligothiophenes, and oligoacenes of varying lengths. For the alkanes, ω saturates quickly with the number of repeat units, while for strongly π-conjugated systems such as polyenes and oligoacenes $1/\omega$ grows strongly with chain length. For the oligothiophenes, $1/\omega$ grows linearly for the shorter oligomers but then saturates at around 10 repeat units.

Our results reveal the dependence of the optimal ω values on the π-conjugation of the system. In particular, they clearly show that while the concept of employing just a single system-independent range-separation parameter might yield a reasonable approximation for small and/or saturated molecules, it is doomed to fail dramatically for longer π-conjugated molecules. Hence, the IP-optimization is an unavoidable step when using LRC-hybrids to study π-conjugated materials of interest in organic electronics. This is especially important as the IP-optimized LRC-hybrids clearly outperform all typically employed density functionals when it comes to predicting IPs, electron affinities, and fundamental energy gaps, all of which are among the most studied

material properties. We underscore that the quality of the performance of the IP-optimized LRC-hybrids is in line with previous results on several different observables and systems of different nature.[2,15,17,20,21] Importantly, this approach offers a much more accurate alternative to standard hybrid functionals, while being equally expensive from a computational point of view.

ACKNOWLEDGMENTS

The authors thank Stephan Kümmel, Roi Baer, and Leeor Kronik for illuminating discussions on long-range corrected DFT. This work has been supported by the AFOSR through the COMAS MURI program (Agreement No. FA9550-10-1-0558). T.K. also thanks the Alexander-von-Humboldt Foundation for financial support through the Feodor-Lynen program.

[1] A. Savin and H.-J. Flad, Int. J. Quantum Chem. **5**, 327 (1995).
[2] R. Baer, E. Livshits, and U. Salzner, Annu. Rev. Phys. Chem. **61**, 85 (2010).
[3] Y. Akinaga and S. Ten-no, Chem. Phys. Lett. **46**, 348 (2008).
[4] R. Baer and D. Neuhauser, Phys. Rev. Lett. **94**, 043002 (2005).
[5] J. E. Robinson, F. Bassani, R. S. Knox, and J. R. Schrieffer, Phys. Rev. Lett. **9**, 215 (1962).
[6] A. V. Krukau, O. A. Vydrov, A. F. Izmaylov, and G. E. Scuseria, J. Chem. Phys. **125**, 224106 (2006).
[7] J. Heyd, G. E. Scuseria, and M. Ernzerhof, J. Chem. Phys. **118**(18), 8207 (2003).
[8] J. Heyd, G. E. Scuseria, and M. Ernzerhof, J. Chem. Phys. **124**(21), 219906 (2006).
[9] L. Schimka, J. Harl, and G. Kresse, J. Chem. Phys. **134**, 024116 (2011).
[10] O. A. Vydrov and G. E. Scuseria, J. Chem. Phys. **125**, 234109 (2006).
[11] J. W. Song, T. Hirosawa, T. Tsuneda, and K. Hirao, J. Chem. Phys. **126**, 154105 (2007).
[12] T. M. Henderson, A. F. Izmaylov, G. Scalmani, and G. E. Scuseria, J. Chem. Phys. **131**, 044108 (2009).
[13] H. Iikura, T. Tsuneda, T. Yanai, and K. Hirao, J. Chem. Phys. **115**, 3540 (2001).
[14] H. Sekino, Y. Maeda, M. Kamiya, and K. Hirao, J. Chem. Phys. **126**, 014107 (2007).
[15] A. Karolewski, T. Stein, R. Baer, and S. Kummel, J. Chem. Phys. **134**, 151101 (2011).
[16] T. Stein, L. Kronik, and R. Baer, J. Chem. Phys. **131**, 244119 (2009).
[17] N. Kuritz, T. Stein, R. Baer, and L. Kronik, J. Chem. Theory Comput. **7**, 2408 (2011).
[18] A. Seidl, A. Gorling, P. Vogl, J. A. Majewski, and M. Levy, Phys. Rev. B **53**, 3764 (1996).
[19] T. Körzdörfer and S. Kümmel, Phys. Rev. B **82**, 155206 (2010).
[20] T. Stein, H. Eisenberg, L. Kronik, and R. Baer, Phys. Rev. Lett. **105**, 266802 (2010).
[21] S. Refaely-Abramson, R. Baer, and L. Kronik, Phys. Rev. B **84**, 075144 (2011).
[22] J. D. Chai and M. Head-Gordon, J. Chem. Phys. **128**, 084106 (2008).
[23] T. M. Henderson, J. Chem. Phys. **127**, 221103 (2007).
[24] T. M. Henderson, A. F. Izmaylov, G. E. Scuseria, and A. Savin, J. Chem. Theory Comput. **4**, 1254 (2008).
[25] B. G. Janesko, A. V. Krukau, and G. E. Scuseria, J. Chem. Phys. **129**, 124110 (2008).
[26] A. V. Krukau, G. E. Scuseria, J. P. Perdew, and A. Savin, J. Chem. Phys. **129**, 124103 (2008).
[27] R. Haunschild and G. E. Scuseria, J. Chem. Phys. **132**, 224106 (2010).
[28] T. M. Henderson, B. G. Janesko, and G. E. Scuseria, J. Phys. Chem. A **112**, 12530 (2008).
[29] J. S. Sears, T. Körzdörfer, C.-R. Zhang, and J.-L. Bredas, J. Chem. Phys. **135**, 151103 (2011).
[30] P. Mori-Sanchez, A. J. Cohen, and W. Yang, J. Chem. Phys. **125**, 201102 (2006).
[31] J. P. Perdew, A. Ruzsinszky, G. I. Csonka, O. A. Vydrov, G. E. Scuseria, L. A. Constantin, X. Zhou, and K. Burke, Phys. Rev. Lett. **100**, 136406 (2008).
[32] O. A. Vydrov, G. E. Scuseria, and J. P. Perdew, J. Chem. Phys. **126**, 154109 (2007).
[33] T. M. Henderson, B. G. Janesko, G. E. Scuseria, and A. Savin, Int. J. Quantum Chem. **109**, 2023 (2009).
[34] Y. Shao, L. F. Molnar, Y. Jung, J. Kussmann, C. Ochsenfeld, S. T. Brown, A. T. Gilbert, L. V. Slipchenko, S. V. Levchenko, D. P. O'Neill, R. A. DiStasio, Jr., R. C. Lochan, T. Wang, G. J. Beran, N. A. Besley, J. M. Herbert, C. Y. Lin, T. Van Voorhis, S. H. Chien, A. Sodt, R. P. Steele, V. A. Rassolov, P. E. Maslen, P. P. Korambath, R. D. Adamson, B. Austin, J. Baker, E. F. Byrd, H. Dachsel, R. J. Doerksen, A. Dreuw, B. D. Dunietz, A. D. Dutoi, T. R. Furlani, S. R. Gwaltney, A. Heyden, S. Hirata, C. P. Hsu, G. Kedziora, R. Z. Khalliulin, P. Klunzinger, A. M. Lee, M. S. Lee, W. Liang, I. Lotan, N. Nair, B. Peters, E. I. Proynov, P. A. Pieniazek, Y. M. Rhee, J. Ritchie, E. Rosta, C. D. Sherrill, A. C. Simmonett, J. E. Subotnik, H. L. Woodcock, 3rd, W. Zhang, A. T. Bell, A. K. Chakraborty, D. M. Chipman, F. J. Keil, A. Warshel, W. J. Hehre, H. F. Schaefer III, J. Kong, A. I. Krylov, P. M. Gill, and M. Head-Gordon, Phys. Chem. Chem. Phys. **8**, 3172 (2006).
[35] P. J. Stephens, F. J. Devlin, C. F. Chabalowski, and M. J. Frisch, J. Phys. Chem. **98**, 11623 (1994).
[36] E. Livshits and R. Baer, Phys. Chem. Chem. Phys. **9**, 2932 (2007).
[37] M. A. Rohrdanz, K. M. Martins, and J. M. Herbert, J. Chem. Phys. **130**, 054112 (2009).
[38] A. D. Becke, Phys. Rev. A **38**, 3098 (1988).
[39] T. Tsuneda, T. Suzumura, and K. Hirao, J. Chem. Phys. **110**, 10664 (1999).
[40] J. D. Chai and M. Head-Gordon, Phys. Chem. Chem. Phys. **10**, 6615 (2008).
[41] M. Bendikov, H. M. Duong, K. Starkey, K. N. Houk, E. A. Carter, and F. Wudl, J. Am. Chem. Soc. **126**, 7416 (2004).
[42] B. Hajgato, D. Szieberth, P. Geerlings, F. De Proft, and M. S. Deleuze, J. Chem. Phys. **131**, 224321 (2009).
[43] D. Jiang and S. Dai, J. Phys. Chem. A **112**, 332 (2007).
[44] M. Deleuze, L. Claes, E. Kryachko, and J. François, J. Chem. Phys. **119**, 3106 (2003).
[45] B. Hajgato, M. S. Deleuze, D. J. Tozer, and F. De Proft, J. Chem. Phys. **129**, 084308 (2008).
[46] H. M. Rosenstock, K. Draxl, B. W. Steiner, and J. T. Herron, in *NIST Chemistry WebBook, NIST Standard Reference Database Number 69*, edited by P. J. L. a. W. G. Mallard (National Institute of Standards and Technology, Gaithersburg, MD, 2011).
[47] V. Coropceanu, M. Malagoli, D. A. da Silva Filho, N. E. Gruhn, T. G. Bill, and J. L. Bredas, Phys. Rev. Lett. **89**, 275503 (2002).